

# Design of a Waypoint-tracking Controller for a Biomimetic-autonomous Underwater Vehicle

Jenhwa Guo, Jing-Far Tsai, Forng-Chen Chiu, Sheng-Wen Cheng, Ye-Sheng Ho  
 Dept. of Engineering Science & Ocean Engineering, National Taiwan University  
 73 Chou-Shan Road, Taipei, Taiwan 106 R.O.C.  
 jguo@ntu.edu.tw

**Abstract-** We develop a control system for the waypoint-tracking of a biomimetic-autonomous underwater vehicle (BAUV). The BAUV swims forward by oscillating its body and caudal fin and turns by slanting its body and caudal fin to the side of turning direction. Because of the undulatory motion of BAUV, we take moving averages of swimming velocity and heading error as feedback signal to control the velocity and angular velocity of BAUV. The control algorithm utilizes the oscillating frequency to control the forward speed, and a body-spline offset parameter to control the yawing rate. We verify the effectiveness of control algorithms by experiments. Finally, we discuss the stability of the control system based on a Lyapunov function.

## I. INTRODUCTION

AUVs have great potential for applications in many undersea missions. Traditionally, rotary propellers driven by electric motors power AUVs. But the low efficiency of the small diameter propellers coupled with the large fraction of the hull volume induced positioning, turning and hovering problems. Recently, the integration of engineering and biology provide us a new direction to solve these problems. Fish have great ability to perform precise hovering and agile turning. The shape of fish is suitable for swimming in the water. So we imitate the shape and the motion modes of the fish to develop a prototype AUV. In our previous work, we had established an optimal body-spline for the BAUV to swim forward [1]. In this paper, we combine a turning mode with the forward-swimming mode to design a control system for BAUV's waypoint tracking.

A review of fish swimming modes for aquatic locomotion is presented in [2]. So far, the focus of our BAUV development focused on the control of body and/or caudal fin movements. In the near future, we will include the median and/or paired fins movements to the BAUV system. The turning performance of fish robots is discussed in [3]. Chiu et al. did simulations on undulatory locomotion of a flexible slender body [4]. Chiu analyzed the dynamic characteristics of a BAUV [5]. Guo et al. presented a method to coordinate body segments and paired fins for the BAUV's motion control and guidance [6].

Section II introduces the optimal body-wave equation of BAUV for the forward swimming and the turning. Experimental measurements of BAUV's turning parameter were included in Section II. In Section III, we divided the control system into two levels. The local control level controls the motion of BAUV in the vehicle-fixed

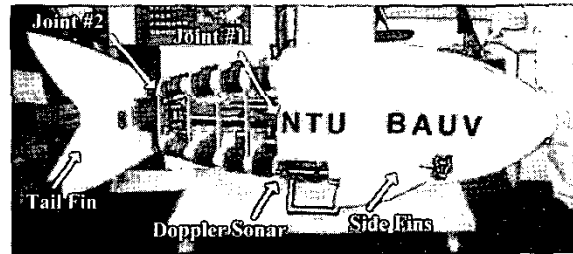


Fig. 1 Photograph of the testbed vehicle

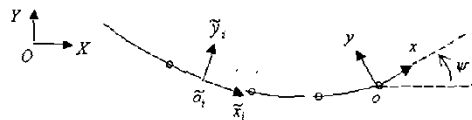


Fig. 2 Definitions of coordinate systems

coordinate. The global control level controls the BAUV to track waypoints in the space-fixed coordinate. The structure of the feedback control system is presented in Section III. Section IV presents experimental results of the waypoint tracking system. Finally, the concluding remarks and future works are given in section V.

## II. FORWARD AND TURNING MOTION

Figure 1 is the outlook of the testbed BAUV. We define three coordinate systems as: space-fixed coordinate system  $O-XY$ , body-fixed coordinate system  $o-xy$  and segment-fixed coordinate system  $o_i-x_i y_i$  shown as in Fig. 2. Each coordinate can be transferred to another by using the relationship of the position and angle between two coordinates.

From observations of fish [8,9], the bodily motion can be considered as traveling waves that increase in amplitude from the nose to the tail. A specific form of traveling wave suggested by Lighthill [9] was

$$f_1(x,t) = f_2(x) \sin(kx + \omega t) \cdot (1 - e^{-\frac{x}{l}}) \quad (1)$$

where

$f_1(x,t)$ : transverse displacement of body

$f_2(x)$ : amplitude envelope; here we define

$$f_2(x) = c_1x + c_2x^2$$

$x$ : displacement along main axis

$k = 2\pi / \lambda$ : body wave number

$\lambda$ : body wave length

$c_1$ : coefficient of linear wave amplitude envelope

$c_2$ : coefficient of quadratic wave amplitude envelope

$\omega = 2\pi f = 2\pi / T$ : frequency

$T$ : period of the body wave

$T_d$ : period of the initial undulating delay cycle

Equation (1) expresses a sinusoidal wave traveling from right to left (i.e. from  $x = 0$  to  $x = -L$ ) within the bounds of a second-order ( $c_1x + c_2x^2$ ) amplitude envelope. The exponential term defining the initial delay when the body starts to undulate is for the convenience of conducting experiments. The slope of the body is  $y_x(x, t) \equiv \partial y / \partial x$ , the angle between the body and the  $x$ -axis is  $\theta \equiv \tan^{-1} y_x$ . From [1], we found that the optimal parameters for our BAUV to swim forward efficiently is  $c_1 = -0.075$ ,  $c_2 = 0.017$ ,  $\lambda = 3.522$ ,  $T = 4$ .

Though real fish turn skillfully using not only tail fin but also pectoral fins or ventral fins, our researches on the BAUV are focused on the tail fin. The turning mode of BAUV is defined as in Fig. 3.

As we know, fish swim by oscillation pattern. They swing their fins and bodies to generate the propulsion force and control the heading direction. Using this turning mode, the BAUV keeps swinging and slanting to one side during turning. We considered it as the most fundamental and important turning mode. One can easily control the turning diameter and forward velocity by this mode.

Since there is no involvement of side fins, it is necessary to keep the swimming speed by oscillating the tail fin, or the BAUV may stop during the turning. We then rewrite the body wave as follow

$$y(x, t) = k_1 \cdot f_1(x, t) + k_2 \cdot f_2(x) \quad (2)$$

where

$y(x, t)$ : transverse displacement of body

$k_1$ : scale factor of the oscillating amplitude

$k_2$ : offset parameter,  $|k_2| \leq 1$

In (2),  $f_1(x, t)$  is the optimal body-wave equation.  $k_2$  controls the magnitude of the center of oscillation away from the nominal position along the BAUV's body. The parameter  $k_2$  controls the offset of BAUV's body spline while the BAUV is turning. For our BAUV, the amplitude of oscillation is restrained by its propulsion mechanism. The parameter  $k_1$  guarantees that joint angles do not exceed their limits.

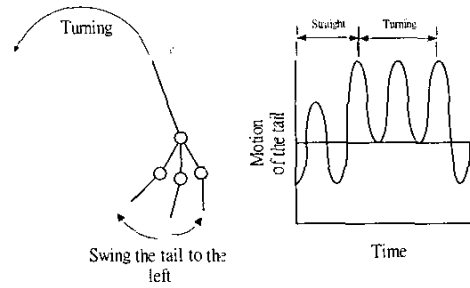


Fig.3 Turning mode of the BAUV

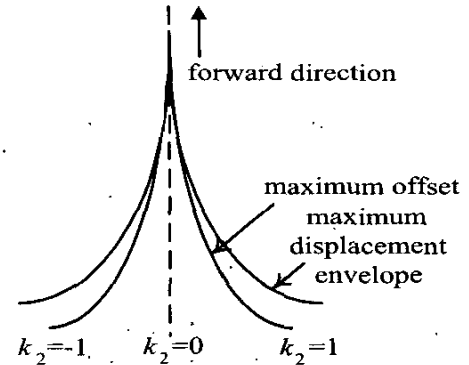


Fig.4 Definitions of  $k_2$

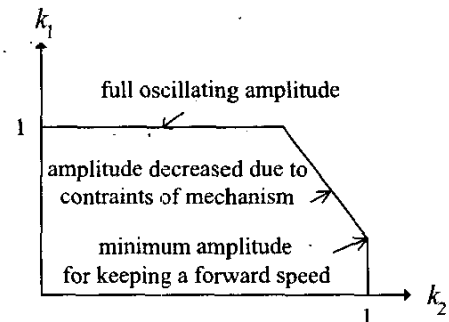


Fig.5 Definition of  $k_1$

The parameter  $k_1$  also keeps the BAUV swimming forward. Their definitions are illustrated in Fig.4 and Fig.5, respectively.

To investigate the characteristics of the BAUV's turning mode, we chose two sets of parameter: Set 1 is  $c_1 = -0.075$ ,  $c_2 = 0.017$ ,  $\lambda = 3.522$ . Set 2 is  $c_1 = -0.094$ ,  $c_2 = 0.031$ ,  $\lambda = 6.51$ . The set 1 data is the optimal body spline obtained from free running experiments using the testbed BAUV [1]. The variables are period ( $T$ ), offset ( $k_2$ ) and forward velocity ( $v$ ). The BAUV is swimming forward using its full oscillating amplitude ( $k_1 = 1$ ).

The model setup is shown in Fig. 6. The BAUV was hung on a three-degree-of-freedom force gauge, which was fixed on a carriage cart above a water tank. The carriage cart

provided constant velocity to the model. The force gauge measured the force in the  $x$  and  $y$  directions together with the moment in the  $z$ -direction.

Figures 7, 8 and 9 are typical data of the experimental results. In this experiment, we set  $T = 4$ ,  $offset = 0$ ,  $v = 0$ . From Fig.10, we observed that the set 1 is a better forward-swimming mode in most of the periods. Figure 11 shows that the set 2 has better yawing moment under the same offset parameter compared to set 1. This is due to the fact that the oscillating envelope of the set 2 is larger than the set 1. Also in Fig.11, we observed that the moment in the  $z$ -direction increased with the value of the offset parameter. The BAUV turns faster with larger offset. In Fig.12, the BAUV had a variable initial velocity, and the higher the initial velocity, the BAUV will turn faster under the same offset. Figures 13 and 14 are results from free running trials using the testbed BAUV in a water tank. The BAUV reached a steady forward speed, then an offset was applied to the body spline. We measured the relationship between the offset values and the yaw rates, sideslip velocities, respectively. It is shown that the offset parameter of the body spline can be used as a direct control factor to modify the yaw rate in a proportional fashion. The offset and the sideslip velocity do not exhibit a proportional relationship.

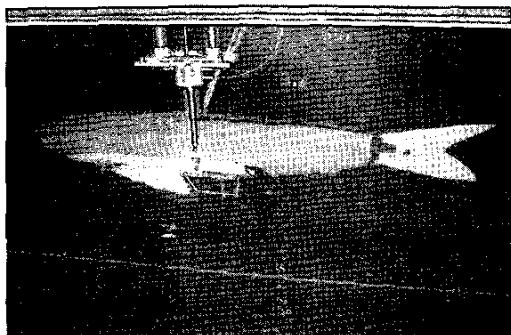


Fig. 6 Model setup for the force and moment measurement

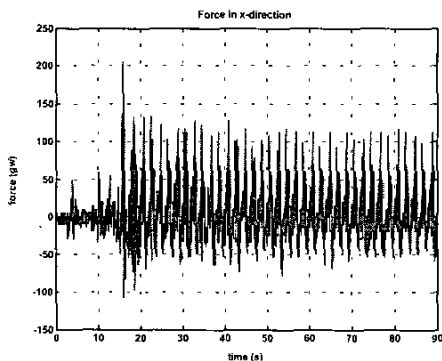


Fig. 7 The force in the  $x$ -direction

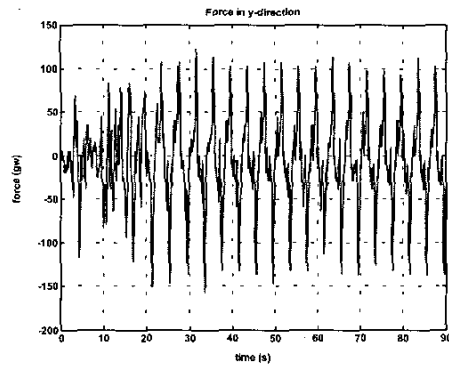


Fig. 8 The force in the  $y$ -direction

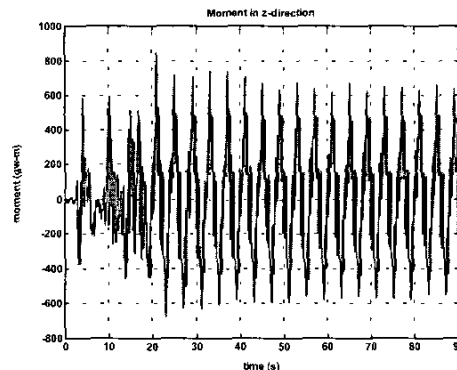


Fig. 9 The moment in the  $z$ -direction

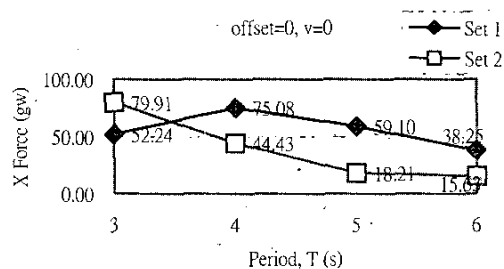


Fig. 10 Force in the  $x$ -direction and oscillation period

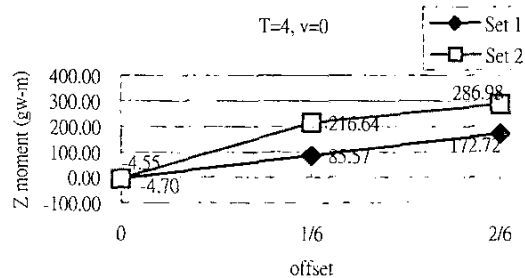


Fig. 11 Moment in the  $z$ -direction and the offset

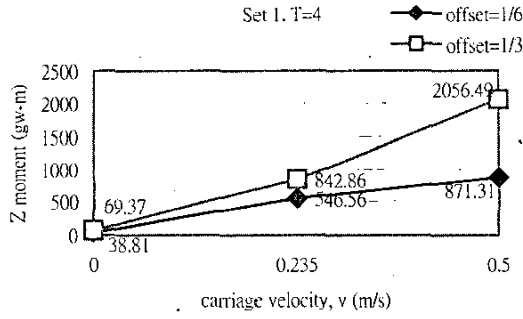


Fig. 12 Moment in the  $z$ -direction with carriage velocity

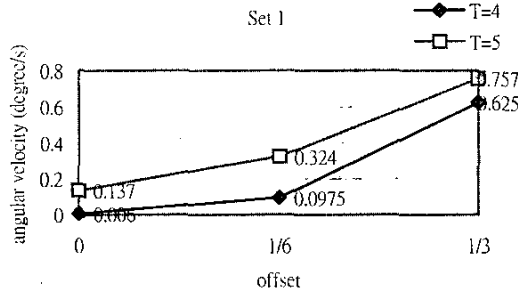


Fig. 13 The relation between offset and angular velocity

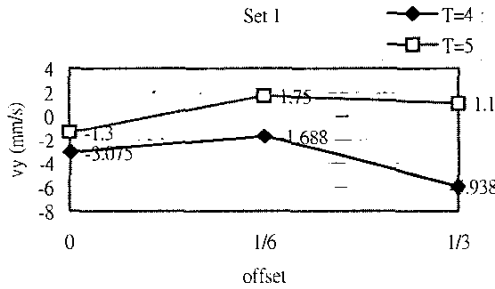


Fig. 14 Offset and the velocity in the  $y$ -direction.

### III. CONTROLLER DESIGN

In this section, we develop a waypoint-tracking control system for the BAUV. Basing on the forward swimming and turning modes we determined in the previous section, by alternating the amplitude and the frequency, we can control the forward velocity of the BAUV. By control the offset parameter, we can control the angular velocity of the turning motion. Because the BAUV moves in an undulating fashion, we take the average of forward speeds, as well as heading errors during the motion period as feedback to control the forward velocity and heading of the BAUV.

Unlike traditional underwater vehicles, BAUVs do not have direct control devices such as thrusters to control the states of BAUVs. The joint angles of BAUV determine the bodily motion, and they move by the interaction forces between the BAUV and the surrounding fluid. The uncertainty of hydrodynamic forces and limitations due to the power supply and mechanical design of the propulsion mechanism make it difficult to precisely control the BAUVs' motion.

In order to overcome the difficulties, we divide the control system to two levels. The local control level generates the oscillation for swimming forward. The global control level controls the performance of waypoint tracking. At the global control level, we let the BAUV track waypoints by evaluate the  $k_2$ . We applied the so-called "line-of-sight" guidance scheme in the horizontal plane. Control error,  $e$ , is defined as the angle between the waypoint and the BAUV in the global coordinate minus the heading angle of the BAUV. Feedback signals are the average of errors in one swimming period. The averaged error is defined as

$$\bar{e} = \frac{\int_{t_0}^{t_0+T} e}{T} \quad (3)$$

where

$\bar{e}$ : averaged error

$e$ : angular difference between the waypoint and BAUV's heading

$T$ : period of body-wave

We take the sum of averaged error and its differentiation and divide the sum by a parameter  $k_e$ .  $k_e$  is responsible for the sensitivity of error correction. The offset  $k_2$  is evaluated by the following equations

$$\begin{cases} k_2 = \frac{\lambda_e \bar{e} + \dot{\bar{e}}}{k_e} & \left| \frac{\lambda_e \bar{e} + \dot{\bar{e}}}{k_e} \right| \leq 1 \\ k_2 = 1 & \frac{\lambda_e \bar{e} + \dot{\bar{e}}}{k_e} > 1 \\ k_2 = -1 & \frac{\lambda_e \bar{e} + \dot{\bar{e}}}{k_e} < -1 \end{cases} \quad (4)$$

where

$\lambda_e$ : coefficient of  $\bar{e}$

$\dot{\bar{e}}$ : differentiation of the averaged error

$k_e$ : coefficient of sensitivity

To show that by using (3) and (4), we can control the BAUV to track waypoints, the following proof is provided.

In Fig. 15, the feedback system is shown in its block diagram form. The following definitions are used

$$e = \psi_d - \psi \quad (5)$$

$$\dot{e} = \dot{\psi}_d - Jq \quad (6)$$

$$\dot{\psi} = Jq \quad (7)$$

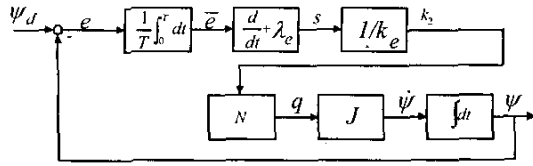


Fig.15 Control system block diagram

where  $\psi$  is the yaw angle in the  $O-XY$ ,  $q$  is the yaw rate in the  $o-xy$ , and  $J=1$  is the transformation from  $o-xy$  to  $O-XY$ .  $N$  represents the transformation from the offset to the yawing rate discussed in the section II.  $N$  is approximately a linear function.

$$s = \left( \frac{d}{dt} + \lambda_e \right) \bar{e} = \frac{1}{T} e + \frac{\lambda_e}{T} \int_0^T e dt = \frac{1}{T} e + \lambda_e \bar{e} \quad (8)$$

$$\dot{s} = \frac{1}{T} \dot{e} + \frac{\lambda_e}{T} e \quad (9)$$

We define a Lyapunov function:

$$V = \frac{1}{2} s^T s \quad (10)$$

The time derivative of the Lyapunov function is

$$\begin{aligned} \dot{V} &= s^T \dot{s} = s^T \left( \frac{1}{T} \dot{e} + \frac{\lambda_e}{T} e \right) \\ &= s^T \left( \frac{1}{T} \right) (\dot{e} + \lambda_e e) = \frac{1}{T} s^T (\dot{\psi}_d - Jq + \lambda_e e) \end{aligned} \quad (11)$$

We design the controller such that

$$q = J^{-1} (\dot{\psi}_d + \lambda_e e + s/k_e) = J^{-1} (\dot{\psi}_d + \lambda_e e + k_2) \quad (12)$$

where  $k_e$  is positive, then

$$\begin{aligned} \dot{V} &= \frac{1}{T} s^T (\dot{\psi}_d - J J^{-1} (\dot{\psi}_d + \lambda_e e + s/k_e) + \lambda_e e) \\ &= \frac{-1}{T} \frac{s^T s}{k_e} \leq 0 \end{aligned} \quad (13)$$

From the above derivations, we can prove that the system is stable in the Lyapunov sense. The fact that the yaw rate,  $\dot{\psi}$ , is linearly dependent on  $k_2$  provides stability to the controlled behaviors of the BAUV.

#### IV EXPERIMENTS

The BAUV has five components: head, caudal part, tail fin, and two pectoral fins. The head segment, tail fin, and pectoral fins are rigid, and the caudal part is supported by a rigid link and some flexible materials. A Doppler sonar is set in the abdominal part of the BAUV for sensing the direction, velocity, and water depth. We focus on body and

caudal fin movements. Pectoral fins are not concerned now, but they will be studied in the near future.

Two cases of waypoint-tracking experiments are illustrated here. In the following experimental setups, case 1 involves results of tracking a single target point. Case 2 provides three waypoints for the BAUV to swim around. These points are at (4,0.5) m, (4,2) m, and (2,2) m. When the distance between the position of BAUV and the target is less than 0.5 m, this waypoint is considered being reached.

We set the parameters as  $c_1 = -0.075$ ,  $c_2 = 0.017$ ,  $\lambda = 3.522$ ,  $T = 4$  sec., and the scale factor  $k_1$  started to decrease at  $k_2 = 0.5$ . That is, the BAUV will decrease its speed for the cases where large offset  $k_2$  is required. The variables to be turned are  $\lambda_e$  and  $k_e$ . In case 1,  $\lambda_e = 2$  and  $k_e = 90$ . Figures 16-26 are outputs of the control system of tracking single waypoints.

For the case 2, the parameters are the same as in the case 1, and the variables to be turned are  $\lambda_e$  and  $k_e$ . Figure 27 shows the results of tracking three waypoints arranged in a way such that large turning maneuvers are required.

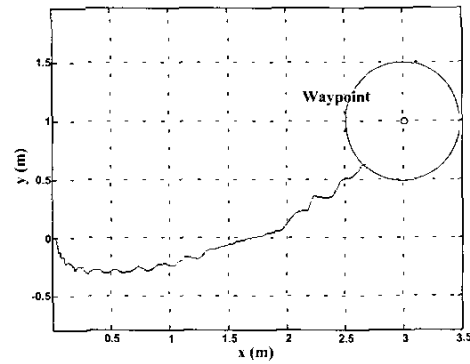


Fig. 16 The swimming path of BAUV,  $\lambda_e = 2$ ,  $k_e = 90$

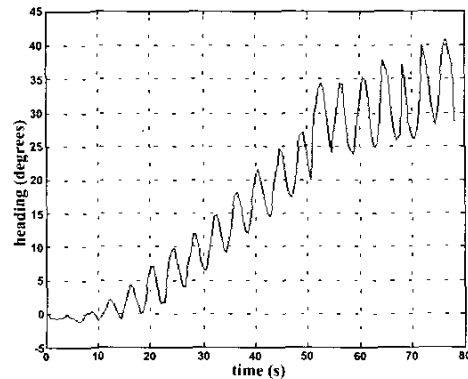


Fig. 17 The heading of BAUV

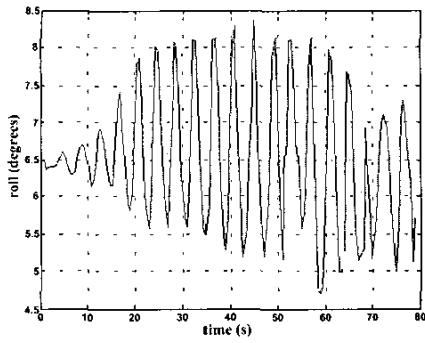


Fig.18 The roll of BAUV

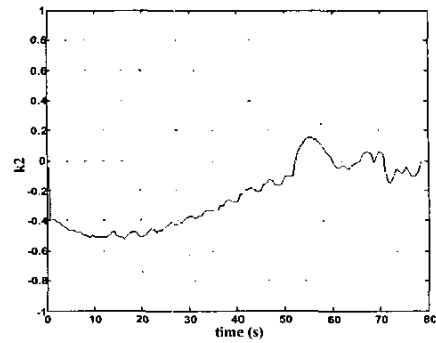


Fig. 22 The offset  $k_2$

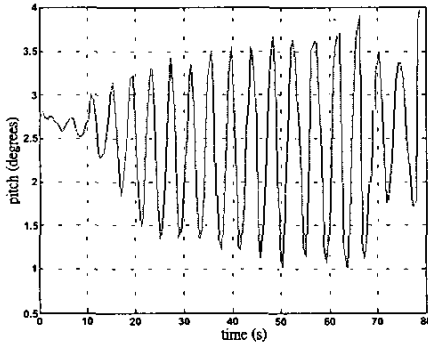


Fig. 19 The pitch of BAUV

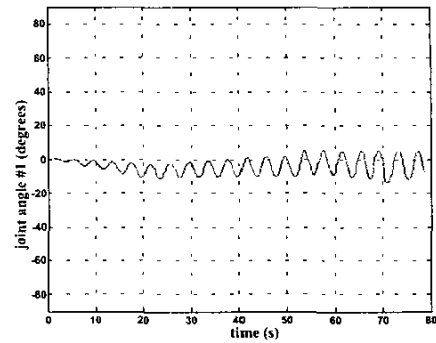


Fig. 23 The joint angle #1

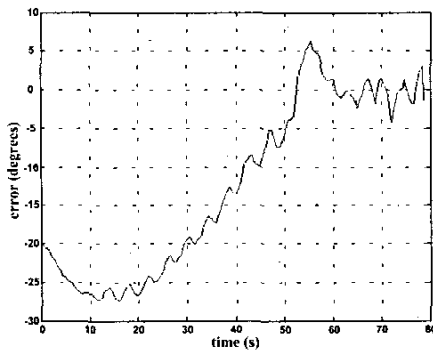


Fig. 20 The error

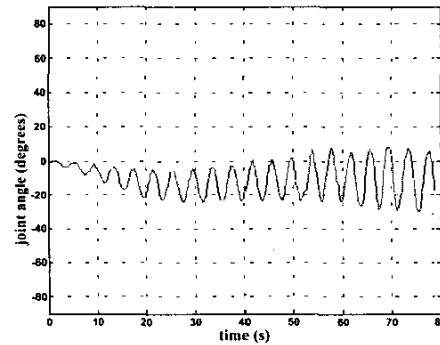


Fig. 24 The joint angle #2

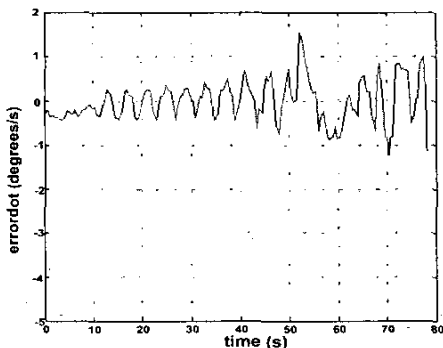


Fig. 21 The error differentiation.

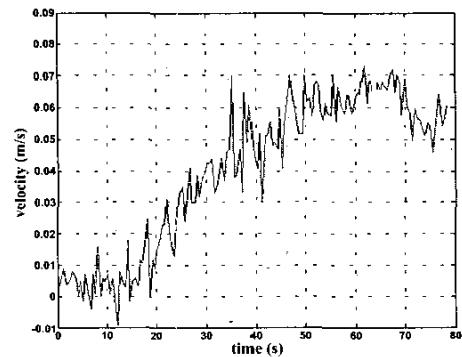


Fig. 25 The velocity in the  $x$ -direction

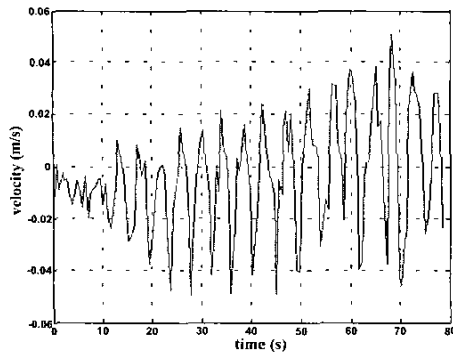


Fig. 26 The velocity in the  $y$ -direction

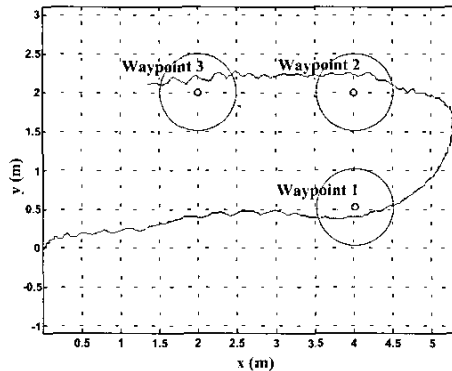


Fig. 27 The tracking of three waypoints

It was observed that the parameter  $k_e$  affects the sensitivity of the control system. If  $k_e$  is too small, the system response tends to be unstable. The time derivative of error helps to improve the stability when the value of  $k_e$  is large. But, if the value of  $k_e$  is small, the time derivative of error makes the system less stable instead.

## V. CONCLUDING REMARKS

To implement waypoint-tracking capability, we propose a way of combining the forward-swimming mode and the turning mode of a biomimetic-autonomous underwater vehicle (BAUV) for the motion control. By alternating the amplitude and frequency of body-wave equation, we can control the forward speed of BAUV. By control an offset parameter of the body spline, we can control the yaw rate directly. Averages of forward speeds and heading errors during the motion period are served as feedback to control the velocity and heading of BAUV. Limits in joint angles of the swimming mechanism were considered in the controller design. We have demonstrated by experiments that our waypoint-tracking controller provides satisfactory tracking capability for the BAUV. The performance of the control system can be adjusted by choosing different control parameters.

To improve the performance of the control system, environmental information can be used to better the

precision of navigation system. More sensors such as vision camera or forward-looking sonar are necessary. To decrease the roll and pitch motions, the balance between buoyancy and weight in every body section shall be considered in the future. The recoil motion decreases swimming efficiency, pectoral fins must be considered in the BAUV control system in the future.

## ACKNOWLEDGMENT

The authors would like to thank the National Science Council of the R.O.C. for financially supporting this research under Contract No. NSC90-2611-002-030.

## REFERENCES

- [1] J.Guo, F.C. Chiu, C.C. Chen, Y.S. Ho, "Determining the bodily motion of a biomimetic underwater vehicle under oscillating propulsion," *Proc. IEEE Int'l Conf. on Robotic and Automation*, Taipei, Taiwan, September 2003.
- [2] M. Sfakiotakis, D. M. Lane, and J. B. C. Davies, "Review of fish swimming modes for aquatic locomotion," *IEEE Journal of Oceanic Engineering* Vol.24, No 2, pp. 237-252, April 1999.
- [3] K. Hirata, T. Takimoto, and K. Tamura, "Study on turning performance of a fish robot," *Proc. the 1<sup>st</sup> International Symp. on Aqua Bio-Mechanisms*, Honolulu, Hawaii, pp.287-292, August 2002.
- [4] F.C. Chiu, C.P. Wu, J.Guo, "Simulation on the undulatory locomotion of a flexible slender body," *Proc. The 1<sup>st</sup> International Symp. on Aqua Bio-Mechanisms* pp.185-190, Hawaii, U.S.A., 2000.
- [5] F. C. Chiu, J. Guo, J. G. Chen, Y. H. Lin, "Dynamic characteristic of a biomimetic underwater vehicle," *UT'02*, Tokyo, Japan, April 2002.
- [6] J.Guo, F. C. Chiu, S.W. Cheng, Y.J. Joeng, "Motion control and way-point tracking of a biomimetic underwater vehicle," *Proc. IEEE Int'l Symp. on Underwater Technology*, Tokyo, Japan, pp. 73-78, 2002.
- [7] J. J. Viedler and F. Hess, "Fast continuous swimming of two pelagic predators, Saithe and Mackel: a kinematic analysis," *Journal of Experimental Biology*, 109, pp.209-228, 1984.
- [8] H. Dewar, *Studies of tropical tuna swimming performance: thermoregulation, swimming mechanics and energetics*, PhD Thesis in Marine Biology, University of California, San Diego, 1993.
- [9] M. J. Lighthill, "Note on the swimming of slender fish," *J. Fluid Mech.*, vol. 9, pp.305-317, 1960.